J Appl Electrochem (2009) 39:1059–1066
DOI 10.1007/s10800-008-9757-2

ORIGINAL PAPER

Effects of surface area on electrochemical performance of $Li[Ni_{0.2}Li_{0.2}Mn_{0.6}]O_2$ cathode material

Jea Hyeok Ryu · Bo Gun Park · Seuk Buom Kim · Yong Joon Park

Received: 20 August 2008 / Accepted: 12 December 2008 / Published online: 24 December 2008

Abstract The effect of surface area on the electrochemical properties and thermal stability of $Li[Ni_{0.2}Li_{0.2}Mn_{0.6}]O_2$ powders was characterized using a charge/discharge cycler and DSC (Differential Scanning Calorimeter). The surface area of the samples was successfully controlled from ~4.0 to ~11.7 $m^2\ g^{-1}$ by changing the molar ratio of the nitrate/acetate sources and adding an organic solvent such as acetic acid or glucose. The discharge capacity and rate capability was almost linearly increased with increase in surface area of the sample powder. A sample with a large surface area of 9.6–11.7 $m^2\ g^{-1}$ delivered a high discharge capacity of ~250 mAh g^{-1} at a 0.2 C rate and maintained 62–63% of its capacity at a 6 C rate versus a 0.2 C rate. According to the DSC analysis, heat generation by thermal reaction between the charged electrode and electrolyte was not critically dependent on the surface area. Instead, it was closely related to the type of organic solvent employed in the fabrication process of the powder.

Keywords Chemical synthesis · Electrochemical measurement · Electrochemical properties · Lithium battery · Cathode · Surface area

J. H. Ryu · B. G. Park · S. B. Kim · Y. J. Park
Department of Advanced Materials Engineering, Kyonggi University, Suwon, Gyeonggi-do 443-760, South Korea

Y. J. Park (✉)
Division of Advanced Industrial Engineering, Kyonggi University, San 94-6, Yiui-dong, Yeongtong-gu, Suwon, Gyeonggi-do 443-760, South Korea
e-mail: yjpark2006@kyonggi.ac.kr

1 Introduction

Lithium secondary batteries have served as key components of cellular phones, PDAs, and lap-top computers for >15 years. They have also recently been investigated as a possible power source for new applications such as electric vehicles (EVs), hybrid electric vehicles (HEVs), and electric power tools [1–3]. In order for these batteries to be used in new application fields, high rate capability will be an important factor due to the necessity of a fast charge/discharge reaction. In particular, the rate performance of the cathode material appears to be the bottleneck in the development of lithium secondary batteries with high rate capability. Therefore, a variety of methods to improve the rate performance of the cathode material have been proposed, such as doping of another transition metal [4, 5], addition of a conductive substance such as carbon [6–8] or metal powder [9–11], and decreasing the particle size and/or increasing the surface area [12–20]. Among these methods, extending the surface area of the cathode powder is an ideal means of increasing the activity of the electrode, because there is no capacity loss due to additives for increasing conductivity. It is expected that extension of the specific surface area of the cathode powder would accelerate the diffusion of lithium ions between the electrode and electrolyte, thereby improving the rate capability of the lithium secondary battery. However, the effect of surface area on the electrochemical properties has been little reported except a few articles [16, 18].

Herein, we investigated the effect of surface area on electrochemical properties of $Li[Ni_{0.2}Li_{0.2}Mn_{0.6}]O_2$ prepared by a simple combustion method. $Li[Ni_{0.2}Li_{0.2}Mn_{0.6}]O_2$ is a promising cathode material with a high discharge capacity of >200 mAh g^{-1} and stable cyclic performance [21–24]. Surface area of the sample powders was controlled by

changing the molar ratio of nitrate/acetate sources and adding an organic solvent. The simple combustion method used for preparing the samples in this work is sufficiently exothermic to drive a redox reaction between the nitrates and acetates. Nitrate source materials such as nickel(II) nitrate hexahydrate and lithium nitrate work as an oxidizing agent as well as a gelling agent. In contrast, the acetate source material acts as a fuel under mixing with the oxidizing powder of the nitrate source. Once ignition occurs, thermal decomposition spontaneously occurs over the reactants, since the fuel (acetate sources) closely coexists with the oxidizing agent (nitrate sources) in a homogeneously mixed state. At this point, the intensity of the production of the gases is a key factor in controlling the particle size and surface area [21].

We attempted to control the surface area of the samples by changing the ratio of nitrate/acetate sources (oxidizing agent/fuel). In some samples, acetic acid and glucose, which may work as a gelating agent and fuel, under a combustion reaction, were also added as an organic solvent to control the surface area of the powders.

In this paper, the main focus of the investigation was on the influence of surface area on rate performance. The discharge capacity and cyclic performance were observed as the charge-discharge rate was increased from 0.2 to 6 C. A DSC analysis was also carried out to investigate the thermal stability of $Li[Ni_{0.2}Li_{0.2}Mn_{0.6}]O_2$ cathode material with various surface areas.

2 Experimental

$Li[Ni_{0.2}Li_{0.2}Mn_{0.6}]O_2$ was prepared by a simple combustion method from manganese acetate tetrahydrate $[Mn(CH_3CO_2)_2 \cdot 4H_2O]$, nickel(II) nitrate hexahydrate $[Ni(NO_3)_2 \cdot 6H_2O]$, lithium nitrate $[LiNO_3]$, and lithium acetate dihydrate $[CH_3CO_2Li \cdot 2H_2O]$. Firstly, stoichiometric amounts of source materials were dissolved in solvents and continuously stirred at 80–90 °C on a hot plate. The amount of sources and solvent for preparing five samples were listed in Table 1. To control the surface area of the samples, the molar ratio of Li nitrate/Li acetate dihydrate was adjusted 1/1, 2/1, 1/2, 1/0. Acetic acid or glucose was added as an organic solvent for more gas generation with or without distilled water. As the solvent evaporated, the mixed solution turned into a viscous gel. The gel was fired at 400 °C for 1 h and a vigorous decomposition process occurred resulting in an ash-like powder. The decomposed powder was ground and heated at 500 °C for 3 h. The obtained powder was reground and heated at 800 °C in air for 7 h. Then, it was quenched to room temperature. The five samples obtained in this manner are hereafter named SA-10 (Sample obtained with *A*cetic acid solvent and source ration of Li nitrate:Li acetate = 1:0), SW-12 (Sample obtained with distilled-Water solvent and source ration of Li nitrate:Li acetate = 1:2), SA-21(Sample obtained with Acetic acid solvent and source ration of Li nitrate:Li acetate = 2:1), SA-11 (Sample obtained with Acetic acid solvent and source ration of Li nitrate:Li acetate = 1:1), and SG-10 (Sample obtained with Glucose solvent and source ration of Li nitrate:Li acetate = 1:0).

The surface area of those powders was determined by BET (Brunauer-Emmett-Teller) analysis using a surface area and porosity analyzer (Micromeritic, ASAP 2010). X-ray diffraction (XRD) patterns of powders were obtained using a Philips X-ray diffractometer in the 2θ range of 15°–70° with monochromatized Cu-K_α radiation (l = 1.5406 Å). The microstructure of the powder was observed using a FESEM (field-emission scanning electron microscopy, JEOL-JSM 6500F).

Electrochemical measurements were performed in a pouch cell, consisting of $Li[Ni_{0.2}Li_{0.2}Mn_{0.6}]O_2$ cathodes and lithium metal anode separated by a microporous polyethylene film. For the preparation of the cathode electrode, 0.32 g of polyvinyl difluoride (Aldrich), 3.2 g of the sample powder and 0.48 g of Super P black (MMM Carbon Co.) were mixed with 16–22 mL of *N*-methyl-2-pyrrolidone by ball milling system. After 24 h of ball mill processing, the viscous slurry was coated onto aluminum foil using a doctor blade then, dried at 90 °C in an oven. The obtained cathode film was pressed. The thickness of the cathode film was about 30 μm. The electrochemical cell was assembled in a dry room using above cathode material. We used a 1 M $LiPF_6$ solution in 1:1 volumetric

Table 1 The used moles of starting material

Sample	$LiNO_3$	$Li(CH_3COO)_2$	$Ni(NO_3)_2$	$Mn(CH_3COO)_2$	$C_6H_{12}O_6$	CH_3COOH	D.I. Water
SA-10	0.24	0.00	0.04	0.12	0.00	1.00	Not used
SW-12	0.08	0.16	0.04	0.12	0.00	0.00	Used
SA-21	0.16	0.08	0.04	0.12	0.00	1.00	Not used
SA-11	0.12	0.12	0.04	0.12	0.00	1.00	Not used
SG-10	0.24	0.00	0.04	0.12	0.333	0.00	Used

ratio of ethylene carbonate/dimethyl carbonate as electrolyte. Cells were subjected to galvanostatic cycling using a Toyo charge-discharge system in the voltage range of 4.8–2.0 V at various constant current density of 40–1,200 mAg^{-1}. DSC samples for the cathode were prepared by following treatment before test. The cells containing sample electrode was charged to 4.8 V at the current density of 40 mAg^{-1}, and it was held at that potential until the current density reached 4 mAg^{-1}. Then these cells were disassembled in a dry room to remove the charged positive electrode. 4.7 mg of the positive electrode (3.76 mg of cathode powder) and 3 μL of fresh electrolyte were sealed in a high pressure DSC pan. The heating rate and temperature range of the DSC tests were 5 °C min^{-1} and 25–300 °C, respectively.

3 Results and discussion

Figure 1 shows XRD patterns of $Li[Ni_{0.2}Li_{0.2}Mn_{0.6}]O_2$ powders synthesized with various molar ratios of nitrate/acetate sources and the addition of an organic solvent.

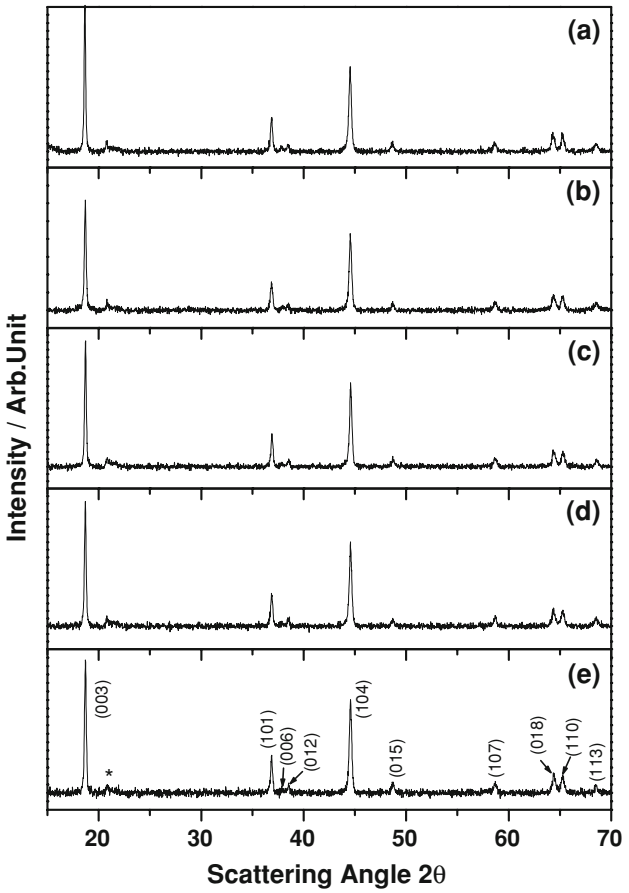

Fig. 1 XRD patterns of $Li[Ni_{0.2}Li_{0.2}Mn_{0.6}]O_2$ powders. **a** SA-10, **b** SW-12, **c** SA-21, **d** SA-11, **e** SG-10. The *star* (*) indicates the superlattice ordering peak

Table 2 Lattice parameters and surface area of $Li[Ni_{0.2}Li_{0.2}Mn_{0.6}]O_2$ samples

Sample	*a*-axis (Å)	*c*-axis (Å)	*c/a*	Surface area (m^2 g^{-1})
SA-10	2.859	14.283	4.996	4.01
SW-12	2.859	14.279	4.994	7.31
SA-21	2.859	14.291	4.999	8.44
SA-11	2.859	14.274	4.993	9.63
SG-10	2.861	14.271	4.998	11.71

Small XRD peaks between 20 and 25° (marked as *) are attributed to superlattice ordering of Li and Mn in the transition-metal containing layers [21–23]. Except for the superlattice ordering peaks, the diffraction patterns of the five samples are indexed well with that of a hexagonal α-$NaFeO_2$ structure (space group R-3m). There is no evidence of a special phase change that could be attributed to the molar ratio of the sources or addition of the organic solvent. Table 2 presents the lattice parameters and surface area of the five samples. The lattice parameters appear to be affected by the conditions of the starting materials. However, both *a* and *c* parameters were within the range of values reported in the literature [21, 24]. The *c/a* ratio of the samples was 4.993–4.999. This also reflects the successful formation of a layered structure under all conditions of the starting materials, as a typical layer structure has a *c/a* ratio higher than 4.899 [25].

As expected, the surface area of the samples was dominantly changed by the molar ratio of the source materials. SA-11 exhibited a high surface area of 9.63, which is more than twofold higher than that of SA-10 (4.01 m^2 g^{-1}), although they were produced under the same heating conditions and with the same organic solvent (acetic acid). Generally, a powder with high surface area can be easily prepared by decreasing the heat-treatment temperature. However, this method adversely impacts the electrochemical properties such as the discharge capacity and cyclic performance, because it can result in products with poor crystallinity, a high concentration of defects and undesired phases by insufficient heat treatment (unstable structure) [26]. Considering that all samples underwent the same heat treatment conditions (800 °C, 7 h), controlling the molar ratio of nitrate/acetate sources is an effective means of obtaining $Li[Ni_{0.2}Li_{0.2}Mn_{0.6}]O_2$ powder with various surface areas. It is expected that a suitable ratio of nitrate (oxidizing agent)/acetate (fuel) sources promotes an increase of gas generation during the combustion process of gel, a reduction of particle aggregation, and increase of surface area. In our work, a 1:1 molar ratio of Li nitrate/Li acetate sources (the total molar ratio of nitrate/acetate, containing Li, Ni, Mn sources, is 2:3) provides the maximum powder surface area when acetic acid is used as an organic solvent.

However, from the point of view of increasing the surface area, further experiments must be conducted to determine the optimum conditions.

Another interesting observation is that the addition of an organic solvent such as glucose or acetic acid remarkably affected the surface area of the samples under the same molar ratio of the sources. As shown in Table 1, the molar content of the organic solvents used for fabrication of SA-10 and SG-10 was adjusted to offer the same content of 'C' and 'H', which may act as fuel in the combustion reaction, in both samples. That is, threefold higher acetic acid (CH_3COOH, containing two C and four H) content in terms of molar ratio than that of glucose ($C_6H_{12}O_6$, containing six C and twelve H) was added to SA-10, under the same content of Li, Ni, and Mn sources. However, the surface area of SG-10 (11.71 $m^2\ g^{-1}$) was about three times greater than that of SA-10 (4.01 $m^2\ g^{-1}$). This clearly shows that the organic solvent not only acts as a fuel but also plays an important role in controlling the surface area.

Figure 2 presents scanning electron microscopy (SEM) images of the $Li[Ni_{0.2}Li_{0.2}Mn_{0.6}]O_2$ powders. The particles appear to be several micrometers in size. In can be seen in the more highly magnified image in the right side of Fig. 2 that each particle consists of aggregates of small primary particles. It appears that the primary particles of SA-10, which has a small surface area of 4.01 $m^2\ g^{-1}$, are tightly connected to each other (Fig. 2a). The particle shape resembles the sintered state of primary particles. Meanwhile, the samples with high surface area such as SG-10 (11.71 $m^2\ g^{-1}$) and SA-11 (9.63 $m^2\ g^{-1}$) appear to be composed of relatively loosely aggregated primary particles. Considerable vacant space is also observed between the primary particles. The weakly connected primary particles appear to be easily pulverized during the mixing process for fabricating the electrode. Moreover, the vacant spaces between particles are expected to increase the contact area between the active material and electrolyte, and thereby facilitate diffusion of lithium ions and charge transport, which would enhance the rate capability of the cell.

To investigate the effect of the surface area of $Li[Ni_{0.2}Li_{0.2}Mn_{0.6}]O_2$ powders on the rate performance, the discharge capacity and cyclic performance were measured at various C rates in a voltage range of 4.8–2.0 V. As mentioned in references [21–24], the $Li[Ni_{0.2}Li_{0.2}Mn_{0.6}]O_2$ compound shows a flat voltage plateau at 4.4–4.6 V in the initial charge process region due to irreversible reaction. To remove the effect of irreversible reaction at the 1st cycle, all the test cells were initially charged and discharged at 0.2 C rate and then cycled at 0.2, 1, 3 and 6 C rates, respectively. Here, the electrochemical data is described from the 2nd cycle and the initial cycle is neglected.

Figure 3a presents the 2nd charge-discharge profiles of cells containing $Li[Ni_{0.2}Li_{0.2}Mn_{0.6}]O_2$ electrodes at 0.2 C rate ($I = 40\ mAg^{-1}$). SA-11 and SG-10 with large surface area showed high discharge capacity of 247 and 257 mAh g^{-1}, respectively. However, the samples with relatively small surface area provided somewhat low discharge capacity (237–241 mAh g^{-1}). This indicates that the surface area of the sample can influence the discharge capacity, even when the charge/discharge rate is very slow (0.2 C). The cyclic performances of the cells containing $Li[Ni_{0.2}Li_{0.2}Mn_{0.6}]O_2$ electrodes are presented in Fig. 3b (0.2 C rate). The discharge capacity of the SA-11 sample

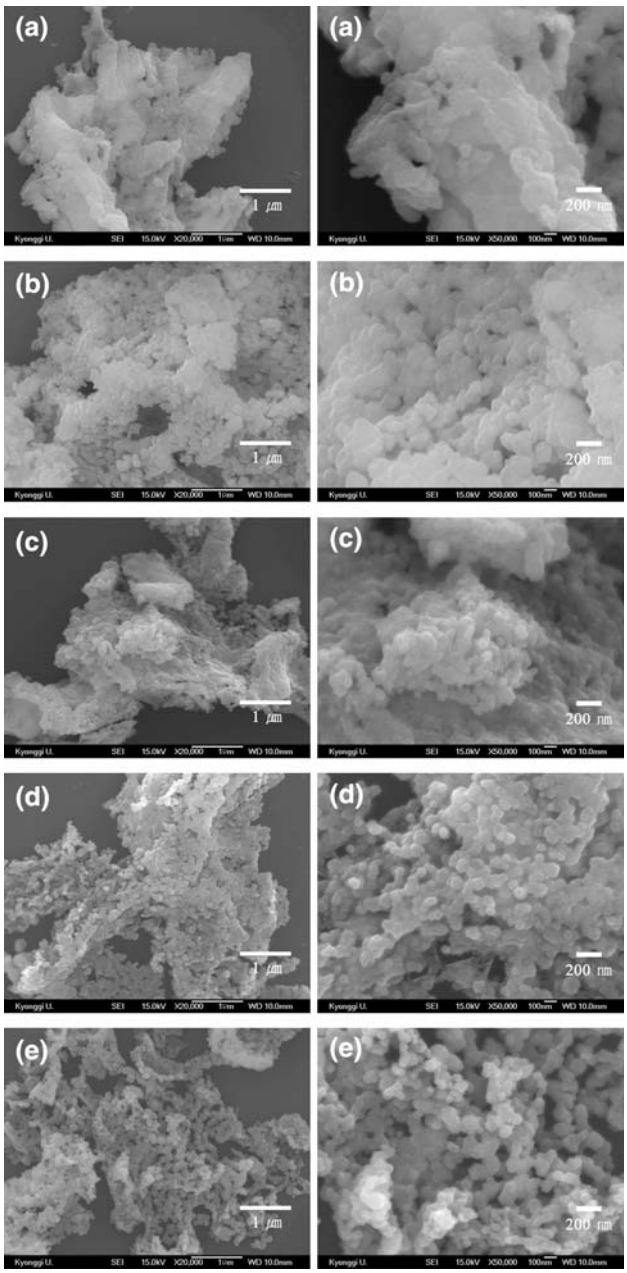

Fig. 2 SEM images of $Li[Ni_{0.2}Li_{0.2}Mn_{0.6}]O_2$ powders. **a** SA-10, **b** SW-12, **c** SA-21, **d** SA-11, **e** SG-10

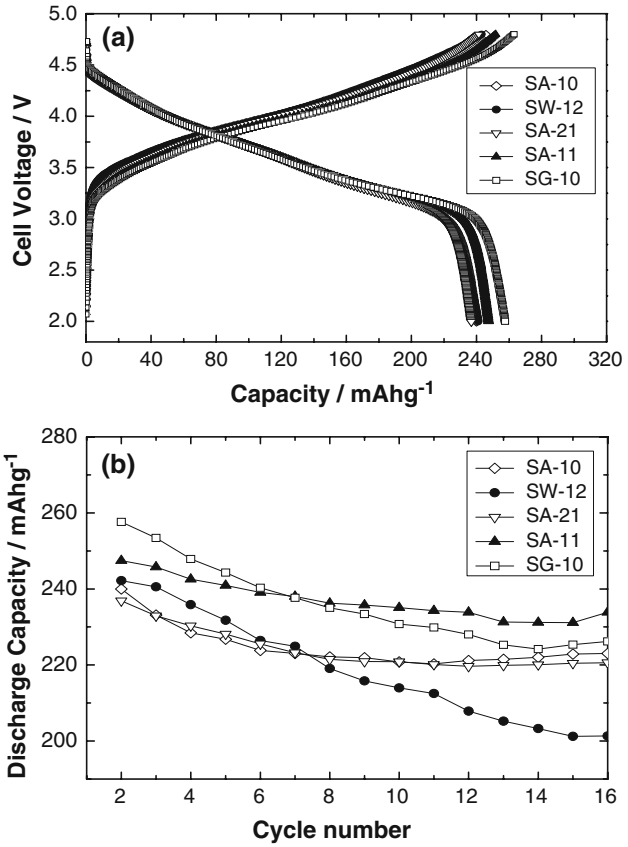

Fig. 3 Electrochemical properties of Li/Li[$Ni_{0.2}Li_{0.2}Mn_{0.6}$]O_2 cells cycled between 4.8 and 2.0 V at a specific current density of 40 mAh g^{-1} (0.2 C rate). **a** Charge/discharge profiles (2nd cycle); **b** Cyclic performance

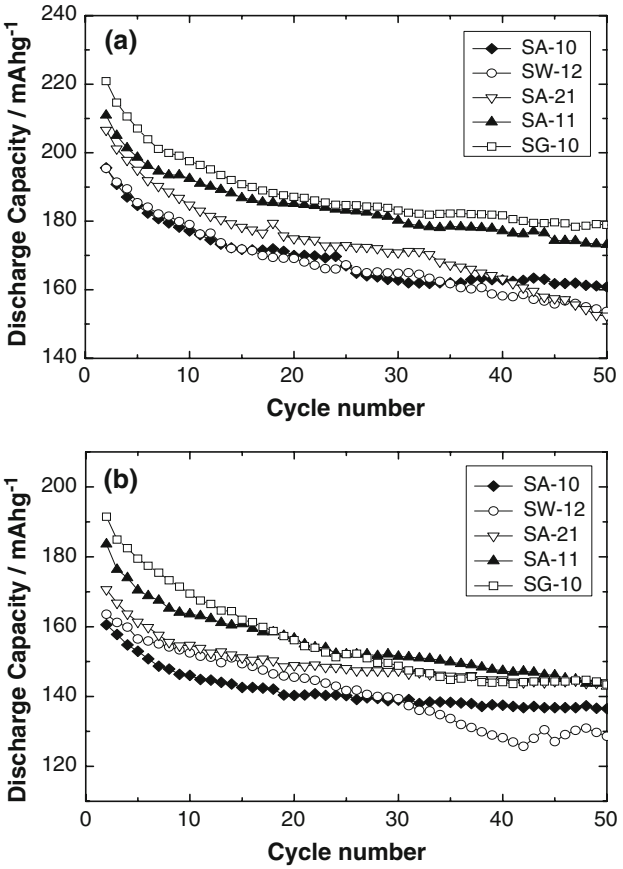

Fig. 4 Cyclic performance of Li/Li[$Ni_{0.2}Li_{0.2}Mn_{0.6}$]O_2 cells cycled between 4.8 and 2.0 V at a specific current of **a** 200 mAh g^{-1} (1 C rate) and **b** 600 mAh g^{-1} (3 C rate)

after 15 cycles (16th cycle) was 234 mAh g^{-1}, which is 94.7% of the 2nd discharge capacity. SG-10 showed a higher 2nd discharge capacity than that of SA-11, but the capacity loss was so large that only 87.6% of the 2nd discharge capacity was maintained after 15 cycles.

Figure 4 shows the discharge capacity (2nd cycle) and cyclic performance of cells containing Li[$Ni_{0.2}Li_{0.2}Mn_{0.6}$]O_2 electrodes at 1 C ($I = 200$ mAg^{-1}) and 3 C ($I = 600$ mAg^{-1}) rate. At both C rates, the discharge capacity of the cells increased almost linearly with increase in the surface area of the sample powder. SA-10 displayed a relatively small discharge capacity of 196 and 136 mAh g^{-1} at 1 and 3 C rate, respectively. While, SG-10 with three times greater surface area (11.71 m^2 g^{-1}) than SA-10 (4.01 m^2 g^{-1}) delivered higher discharge capacity of 221 and 190 mAh g^{-1} at 1 and 3 C rate, respectively. The effect of surface area was more prominently observed at a high charge-discharge rate of 6 C. Figure 5 shows the charge-discharge profile (2nd cycle) and cyclic performance of the Li[$Ni_{0.2}Li_{0.2}Mn_{0.6}$]O_2 electrodes at a 6 C rate. The discharge capacity of SA-10 was 125 mAh g^{-1}, which is only 78% that of SG-10 (161 mAh g^{-1}).

Table 3 summarizes the discharge capacity and capacity retention at various C rates. It is apparent that the ratio of the discharge capacity (2nd cycle) at a rate of 6/0.2 C is highly dependant on the surface area of the powder. As expected, as the surface area of the sample powder was increased, greater capacity was maintained at a high C rate. The ratio of the discharge capacity at 6/0.2 C rate for SA-10 with small surface area is only ~52%. However, the discharge capacity of the sample with high surface area (SA-11) at 6 C rate is >63% than that of samples at a 0.2 C rate, indicating that the rate capability at 6/2 C is enhanced by >20% by increasing the surface area.

Figure 6 presents the surface area versus discharge capacity (2nd cycle) of a cell containing Li[$Ni_{0.2}Li_{0.2}Mn_{0.6}$]O_2 electrodes at various C rates. The graph clearly shows that the discharge capacity increases almost linearly with increase in surface area at all measurement conditions. However, because the samples were prepared with different molar ratios of source materials and solvent, it is possible that other factors except surface area may affect the electrochemical properties of samples. For example, if there is remaining residual carbon originating from the organic

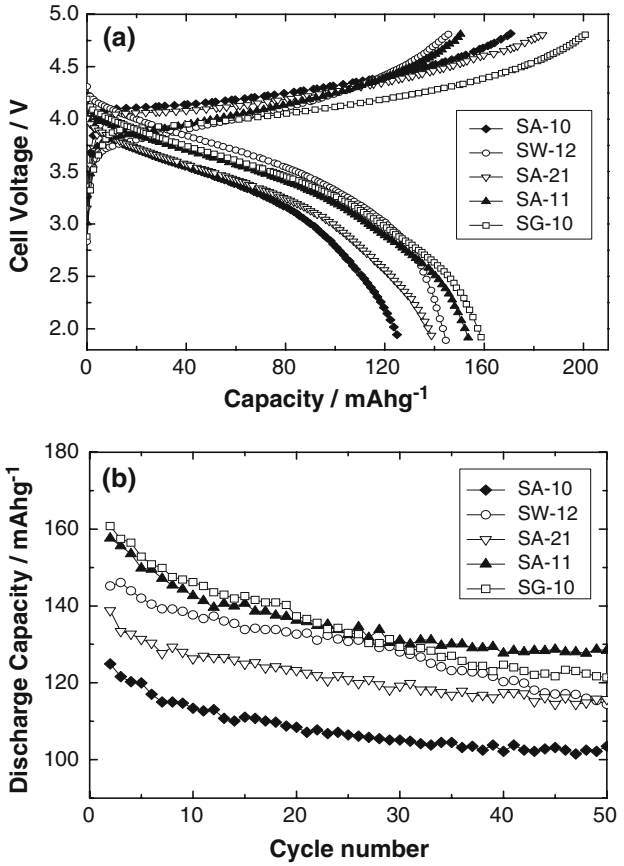

Fig. 5 Electrochemical properties of Li/Li[$Ni_{0.2}Li_{0.2}Mn_{0.6}$]O_2 cells cycled between 4.8 and 2.0 V at a specific current density of 1,200 mAh g^{-1} (6 C rate). **a** Charge/discharge profiles (2nd cycle); **b** Cyclic performance

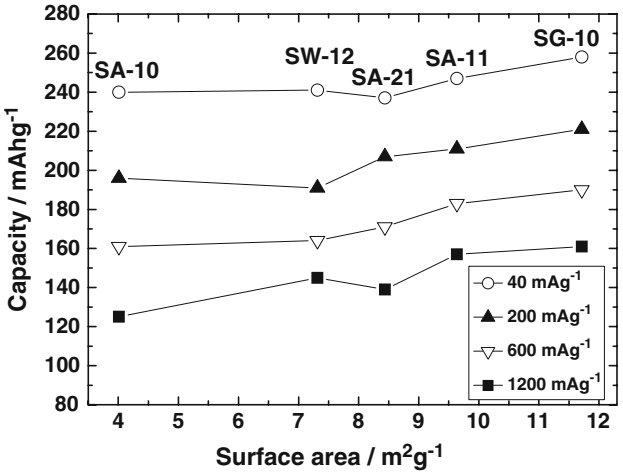

Fig. 6 Surface area of Li[$Ni_{0.2}Li_{0.2}Mn_{0.6}$]O_2 powders versus discharge capacities of the Li/Li[$Ni_{0.2}Li_{0.2}Mn_{0.6}$]O_2 cells cycled between 4.8 and 2.0 V at various specific current densities

solvent, then the capacity and rate capability could be improved due to an increase in electrical conductivity. However, as shown in Fig. 6 and Table 3, SW-12 displays better capacity and rate capability than SA-10, which is prepared with an organic solvent (acetic acid). Considering that SW-12 was synthesized without an organic solvent, it can be concluded that residual carbon is not a more dominant factor with respect to the electrochemical property than surface area. While other factors originating from differences in the starting material cannot be completely ignored, they do not appear to play a role in the observed effect of surface area in the present samples.

Based on the above experiment, it is clear that increasing the surface area of a cathode powder by controlling the starting materials is an effective means of improving the rate capability of a cell. As reported by several authors [16, 18], a large sample surface area makes the electrolyte accessible to a wider region of the active material, and hence it can enhance the rate capability of the cell. Moreover, this phenomenon will be more prominent at much faster charge/discharge rates. It also possible that the high surface area helps drive the phase transformation during the initial charge process more efficiently to fuller completion. This can increase subsequent initial discharge capacity. However, it is suspected that a large cathode surface area may be accompanied by some disadvantages such as degrading of the cycle life and thermal stability of the electrode. First, it is likely that increased interaction of the interlayer region between the active material and electrolyte results in increased dissolution of metal ions and surface reaction with the electrolyte, which may lead to unstable cyclic performance. In this regard, the sample with the highest surface area

Table 3 Discharge capacity and rate capability of Li[$Ni_{0.2}Li_{0.2}Mn_{0.6}$]O_2 samples at various specific current densities

Sample	40 mAg^{-1} (0.2 C rate)			200 mAg^{-1} (1 C rate)			600 mAg^{-1} (3 C rate)			1,200 mAg^{-1} (6 C rate)			Rate capability (ratio of capacity at 6/0.2 C rate) (%)
	2nd	16th	16th/2nd (%)	2nd	50th	50th/2nd (%)	2nd	50th	50th/2nd (%)	2nd	50th	50th/2nd (%)	
SA-10	240	223	92.9	196	160	81.6	161	136	84.5	125	103	82.4	52.08
SW-12	241	201	83.4	191	153	83.4	164	129	83.4	145	115	83.4	60.16
SA-21	237	221	93.2	207	152	73.4	171	144	84.2	139	115	82.7	58.65
SA-11	247	234	94.7	211	178	84.4	183	142	77.6	157	129	82.2	63.56
SG-10	258	226	87.6	221	178	80.5	190	142	74.7	161	121	75.2	62.4

(11.71 $m^2\ g^{-1}$), SG-10, did not show good cycle life at all C rates, although it showed high discharge capacity and good rate capability. However, compared with other samples with smaller surface area, SA-11 with a surface area of 9.63 $m^2\ g^{-1}$ showed no unusual degradation of cycle performance. Within the conditions employed in the experiment, a noticeable relation between surface area and cycle life was not observed, but the possibility of such a relationship cannot be ruled out.

Degradation of thermal stability, which can be induced by a large cathode powder surface area, is also a potential disadvantage. Increasing the surface area will facilitate not only intercalation/deintercalation of lithium ions but also thermal reaction between the cathode and electrolyte. The thermal stability of the cathode materials at a charged state is an important factor for practical applications of lithium battery systems. Herein, a DSC analysis was performed to investigate the thermal stability of $Li[Ni_{0.2}Li_{0.2}Mn_{0.6}]O_2$ electrodes with various surface areas. The $Li[Ni_{0.2}Li_{0.2}Mn_{0.6}]O_2$ electrodes were fully charged to 4.8 V before the test and sealed with fresh electrolyte in a high pressure DSC pan.

In the DSC profiles (Fig. 7), SW-12, SA-21 and SA-11 showed similar shapes. The differences in their surface areas are within a small range (7.31–9.63 $m^2\ g^{-1}$). For these three samples, thermal reaction with the electrolyte commenced at roughly 180–190 °C and heat was generated until ~260 °C. Two large exothermic peaks are located at ~230 and 244–245 °C. The small peak around 120–130 °C may be related to decomposition of organic compounds residing at the particle surface. It appears that heat generation by the thermal reaction was somewhat increased with increased surface area, although which accounts for only 5% of the total heat generation. The DSC profile of SA-10 displayed a slightly different shape. The initial exothermic peak was shifted to ~168 °C, which implies that the thermal reaction was started at that temperature. A second exothermic peak was detected ~230 °C and the total heat generation was not substantially smaller than that of the other samples. SG-10 displays better thermal stability than other samples, despite having the largest surface area among the samples in this work. In the DSC profile of SG-10, an exothermic peak was located at 232 °C and heat generation was only 314 J g^{-1}, which is roughly 55% lower than that of SA-11. Considering that SG-10 was prepared with glucose, it is likely that the thermal stability is related with the type of organic solvent. Overall, it appears that the surface area does not critically affect the thermal stability of the sample.

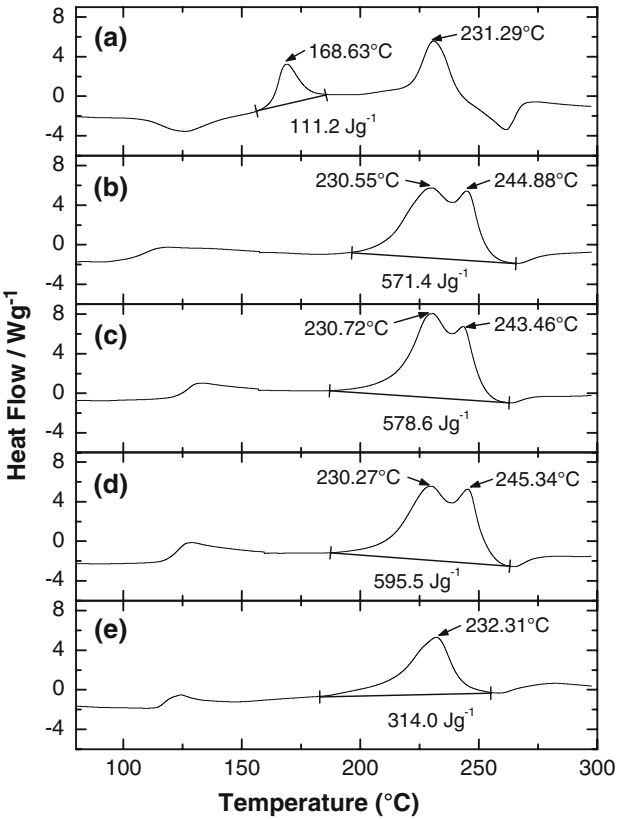

Fig. 7 DSC scans of the $Li[Ni_{0.2}Li_{0.2}Mn_{0.6}]O_2$ cathode at fully charged state (cut off voltage was 4.8 V). The scan rate was 5 °C min^{-1}. **a** SA-10, **b** SW-12, **c** SA-21, **d** SA-11, **e** SG-10

4 Conclusions

$Li[Ni_{0.2}Li_{0.2}Mn_{0.6}]O_2$ powder with various surface areas was successfully synthesized by controlling the molar ratio of the source materials and adding an organic solvent. This method can increase the surface area without decreasing the heat treatment temperature, which can result in degradation of electrochemical properties**.** The discharge capacity and rate capability were remarkably improved by increasing the surface area of the powders. The ratio of discharge capacity at 6/2 C rate is enhanced >20% by increasing the surface area. It is possible that an overly large surface area may adversely affect cycling performance. However, a noticeable relation between surface area and cycle life was not observed in the present experiment. Based on a DSC analysis, the effect of surface area on thermal stability was not critical. However, the organic solvent used for preparation of the gel appears to be strongly related with the thermal stability of the sample.

Acknowledgement This work was supported by the Korean Ministry of Information and Communication (Project No. 2006-S-006).

References

1. Zhang S, Qiu X, He Z, Weng D, Zhu W (2006) J Power Sources 153:350
2. Amine K, Liu J, Belharouak I, Kang SH, Bloom I, Vissers D, Henriksen G (2005) J Power Sources 146:111

3. Huang S, Wen Z, Yang X, Gu Z, Xu X (2005) J Power Sources 148:72
4. Shin Y, Manthiram A (2003) Electrochem Solid State Lett 6:A34
5. Wang X, Tanaike O, Kodama M, Hatori H (2007) J Power Sources 168:282
6. Cushing BL, Goodenough JB (2002) Solid State Sci 4:1487
7. Doeff MM, Wilcox JD, Kostecki R, Lau G (2006) J Power Sources 163:180
8. Kim J, Kim B, Lee J, Cho J, Park B (2005) J Power Sources 139:289
9. Park KS, Son JT, Chung HT, Kim SJ, Lee CH, Kang KT, Kin HG (2004) Solid State Commun 129:311
10. Son JT, Park KS, Kin HG, Chung HT (2004) J Power Sources 126:182
11. Huang S, Wen Z, Yang X, Gu Z, Xu X (2005) J Power Sources 148:72
12. Choi D, Kumta PN (2007) J Power Sources 163:1064
13. Chen H, Qiu X, Zhu W, Hagenmuller P (2002) Electrochem Commun 4:488
14. Kim DH, Kim J (2006) Electrochem Solid State Lett 9:A439
15. Huang H, Yin SC, Nazar LF (2001) Electrochem Solid State Lett 4:A170
16. Xia Y, Yoshio M, Noguchi H (2006) Electrochim Acta 52:240
17. Meligrana G, Gervaldi C, Tuel A, Bodoardo S, Penazzi N (2006) J Power Sources 160:516
18. Kim JS, Johnson CS, Vaughey JT, Hackney SA, Walz KA, Zeltner WA, Anderson MA, Thackeray MM (2004) J Electrochem Soc 151:A1755
19. Leising RA, Palazzo MJ, Takeuchi ES, Takeuchi KJ (2001) J Electrochem Soc 148:A838
20. Maleki H, Hallaj SA, Seiman Jr, Dinwiddie RB, Wang H (1999) J Electrochem Soc 146:947
21. Hong YS, Park YJ, Ryu KS, Chang SH, Kim MG (2004) J Mater Chem 14:1424
22. Lu Z, Dahn JR (2002) J Electrochem Soc 149:A1454
23. Lu Z, Dahn JR (2002) J Electrochem Soc 149:A815
24. Lu Z, Beaulieu LY, Donabberger RA, Thomas CL, Dahn JR (2002) J Electrochem Soc 149:A778
25. Shaju KM, Subba Rao GV, Chowdari BVR (2002) Electrochim Acta 145:151
26. Lee DK, Park SH, Amine K, Bang HJ, Parakash J, Sun YK (2006) J Power Sources 162:1346